

A proposed architecture for convolutional neural networks to detect skin cancers

Hasan Maher Ahmed¹, Manar Younis Kashmola²

¹Software Department, College of Computer Science and Mathematics, University of Mosul, Mosul, Iraq

²Department of Computer Science, College of Computer Science and Mathematics, University of Mosul, Mosul, Iraq

Article Info

Article history:

Received Sep 27, 2021

Revised Jan 26, 2022

Accepted Feb 11, 2022

Keywords:

Basal cell carcinoma
Convolutional neural networks
Deep learning
Melanoma
Nevus

ABSTRACT

The goal of the research paper is to design and development of a computer-based system for the segmentation and classification of malignant skin diseases and a comparison between the accuracy of their detection, as two malignant diseases of skin diseases were detected. Namely, basal cell carcinoma and melanoma separately with images of nevus, and the images were collected from the ISIC 2020 archive group, as the total, The images used: 17,846 images include 3,008 images of basal cell carcinoma (BCC), 5,272 images of melanoma, and 9,566 images of a nevus, and validation data contains 20% of the images used which are not classified and randomly taken from the set of images, and the final test data contains 1,500 anonymous images. An architecture for the convolutional neural network technology in deep learning has been proposed that consists of a set of layers for processing. Processing raw input images for a group of pre-treatment transformations, the data augmentation process, so the number of images used became 86094 images of nevus, 27,072 images of BCC, and 47,448 images of melanoma. Through the detection process, the classification and detection accuracy of BCC was 98.25%, which is higher than the classification accuracy of melanoma is 91.61%.

This is an open access article under the [CC BY-SA](https://creativecommons.org/licenses/by-sa/4.0/) license.



Corresponding Author:

Hasan Maher Ahmed
Software Department, College of Computer Science and Mathematics, University of Mosul
Mosul, Iraq
Email: hasanmaher@uomosul.edu.iq

1. INTRODUCTION

Cancer is the deadliest disease among other diseases. Unfortunately, most cancer patients are diagnosed in the final stages of the disease. The revolution brought about by artificial intelligence in the health sector and other sectors have significantly reduced these risks [1]. Correct diagnosis of diseases is an arduous and time-consuming task that requires many years of medical training. There is a significant shortage of diagnostic experts in many medical specialties. and this places tremendous pressure and a considerable volume of work on the shoulders of doctors in addition to the costs and difficulties faced by patients to reach skilled doctors to diagnose their disease as fast as you can and maybe save their lives [2].

Machine learning is a machine's ability to learn through continuous training of the data set (input) that the algorithm uses and repeats the training process to reach the desired results. Machine learning proves particularly useful when diagnostic information is available in digital forms, such as X-rays, computed tomography (CT) scans, magnetic resonance imaging, skin, and eye images. And deep learning algorithms are characterized by the ability to match patterns in images as they can be trained to detect different types of cancers in CT images [3], [4]. Thanks to artificial intelligence, shortly, all people will be able to reach the

same performance as the best experts in diagnosing diseases based on medical images at a low cost at any time [5].

Skin diseases are characterized by their many shapes, types, and colors, as they form on the surface of the human skin with different textures and colors [6]. When digital images of skin diseases are taken, they are stored in various data in the composition of their textures and color contrast. Many researchers presented research papers in which the distinction of different groups of skin diseases was discussed [7], [8].

Many deep learning architectures appeared [9], such as LeNet architecture [10], [11], which used the detection of benign and malignant tumors. AlexNet architecture appeared [12], [13], which distinguished multiple types of skin diseases and developed the ZFNet algorithm to deal with different types of diseases [14], [15]. The more complex VGG16 and VGG19 architectures were built in the classification operations [16].

2. THE PROPOSED METHOD

The proposed method seeks to design and develop a system based on computer vision to segment and classify skin lesions and extract a distinct set of features from skin lesions for adequate classification. There are many challenges in dealing with digital images of skin taken from digital cameras because they contain noises such as hair and bubbles. These noises are a real obstacle to obtaining accurate classification, and the model will be trained on such noise.

The digital images used were dealt with based on color channels (red, green, blue). And the size of the images was based on 250*250 for each of the basal cell carcinoma and melanoma and nevus. Three channels of the dermatoscopy images (red, green, and blue) are used in each of the convolutional neural networks. Also, work was done to normalize the input images by subtracting the average pixel density and dividing the standard deviation. This treatment makes the mean value of the image become zero, and the standard deviation becomes 1. Images containing hair have been dealt with, which increases the ability to learn and thus improves the testing process.

The images were obtained from the International Skin Imaging Collaboration (ISIC 2020) group, where the ISIC data provides a set of images of skin cancer [17]. The ISIC skin diseases project was implemented to reduce the increased mortality associated with skin cancers and the efficiency of early detection of skin cancer. This ISIC data set contains approximately 69,445 images. Download the training data used in this research from ISIC. The total of 17,846 images of dermatoscopy include 3,008 images of basal cell carcinoma and 5,272 images of melanoma, and 9,566 images of a birthmark, and Figure 1 shows samples of these images, Figure 1(a) sample of basal cell carcinoma, Figure 1(b) sample of melanoma, and Figure 1(c) sample of nevus. The validation data includes 20% of the images used. They are not classified. The final test data contains 1,500 anonymous images. In the ISIC challenge, ultra-pixel images and basic patient information, including age and gender, were presented (in both training and testing, these two criteria were eliminated for patient information) [18], [19].

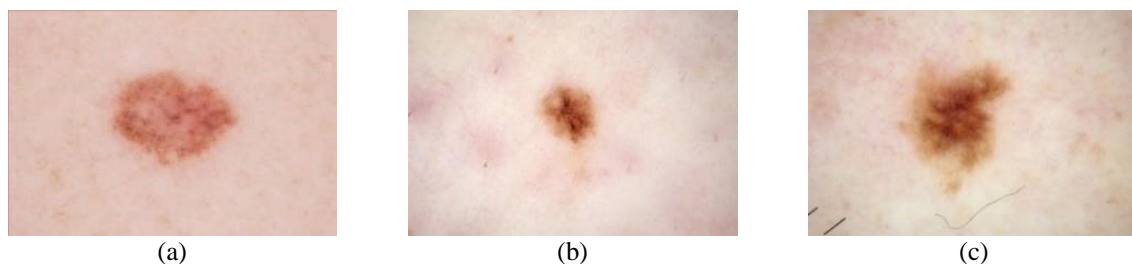


Figure 1. Samples of training images (a) digital color image of a basal cell carcinoma (BCC) sample, (b) digital color image of a melanoma sample, and (c) digital color image of a nevus sample

In this paper, two malignant pathologies of the skin were detected by comparison with the images of nevus. Basal cell carcinoma (BCC) is a malignant skin tumor stemming from skin cancer and is considered the most common form of skin cancer. Basal cells in the skin are small cells usually located in the upper part of the skin (the epidermis layer) [20]. One of the most prominent basal cell carcinoma features is a red spot or an irritated area on the chest, shoulder, arms, and legs. It usually arises on the place, a boil, a shiny bump or a small bright lump or transparent and glossy and sometimes pink, red, or white, and it can also be brown, yellowish, black, or brown and may be confused with a nevus [2], [11].

Melanoma is the deadliest form of skin cancer. Changes in the skin, such as the formation of a mole or a pimple on the skin that grows in size or changes shape over time, as well as the appearance of an abnormally large mole, and the appearance of pale or red pimples on the skin, are all signs of melanoma cancer [12], [13]. The natural nevus has a prominent border that divides the mole from the surrounding skin and is usually a homogenous color such as tan, brown, or black. They are normally oval or spherical, with a diameter of less than a quarter of an inch (approximately 6 mm) when compared to the size of a pencil eraser [3], [15].

When working on specific complex tasks, it is tough to obtain the large amounts of data required to train the models. This problem is solved by applying different transformations to the available data to collect the new data. Figure 2 shows the data augmentation processes wherein Figure 2(a) original images, Figure 2(b) flipping images, Figure 2(c) cropping images, Figure 2(d) apply a Gaussian filter on images, Figure 2(e) Images resizing, Figure 2(f) images rotation by 90°, Figure 2(g) images rotation by 180°, Figure 2(h) images rotation by 270°, and Figure 2(i) images translating.

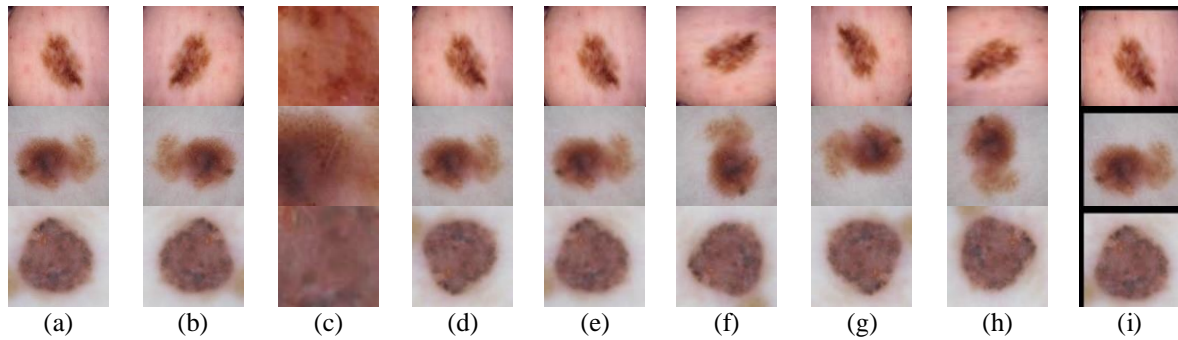


Figure 2. Data augmentation (a) original image, (b) flipping, (c) cropping images, (d) Gaussian filter, (e) images resizing, (f) rotate images by 90°, (g) rotate images by 180°, (h) rotate images by 270°, and (i) images translating

3. ALGORITHM

A convolutional neural network refers to a type of artificial neural network with the main features of a cognitive neural network [17]. The convolutional neural networks (CNN) architecture uses three leading technologies: weight-sharing, local receptor fields, and spatial reduction. This network is somewhat similar to the biological vision system model in that raw data is applied to it as input to the network without the need for primary processing or feature extraction. Feature extraction and identification are performed in a standard structure [19], [20].

Poor lighting conditions can cause images captured in outdoor locations to deteriorate significantly. Low dynamic range and excessive noise levels in these photos can influence the overall effectiveness of computer vision systems. As demonstrated in Figure 3 technology was employed to improve low and high light photos to make the suggested algorithm more powerful in low and high light settings, where is Figure 3(a) Luminous and dark images, Figure 3(b) Invert the Images, and Figure 3(c) apply enhancing algorithm, and Figure 3(d) invert the enhanced images [21]. The process begins with inverting the low-light or high-light image, then applying the optimization algorithm to the inverted image, and then inverting the optimized image as in the following (1) and (2):

$$O(x)=S(x)B(x)+A(1-T(x)) \quad (1)$$

$$J(x)=(O(x)-I_v)/(\max(t(x),t_0))+I_v \quad (2)$$

where O is the observed intensity, S denotes the scene radiance, A denotes ambient light, and T denotes the portion of the light that reaches the camera. Estimating the atmospheric light A using a pre-dark channel, estimating the transmission map T , fine-tuning the estimated transmission map, restoring the image, and optionally conducting contrast enhancement are the steps involved in the enhancement process [22], [23].

Depending on deep learning, work is being done on building an intelligent model for data discovery and classification where the appropriate components can be dragged and dropped to create a suitable model. The proposed model consists of convolutional layers, activating functions, pooling layers, and fully-connected layers as in Figure 4. The digital images were taken consisting of 3 color channels, red, green, and

blue, as this type of digital image gives accurate data to digital images. The depth denotes the number of filters used for the wrapping process. Suppose the warping process is executed on the original image using three different filters (producing three characteristic maps for the input image). In that case, the depth of the properties map will be three [24], [25]. The stride pass-through is the number of pixels used when passing the filter matrix over the input image matrix. When the pass step value is 1, the filter will be moved only one pixel at a time, noting that when the pass-through step size is large, this means that it will produce small-sized character maps [26].

The pooling process reduces the size of spatial inputs continuously and in detail. It represents the inputs in the matrix of properties smaller in terms of the size of the matrix's dimensions. Thus, it is easier to manage and work to reduce the volume of transactions and accounts in the network and thus control overfitting [27], [28]. The network is stable and resistant to minor changes, distortions, and shifts in the input image. It also helps in reaching a representation. That is a powerful feature because it helps identify the objects in the image regardless of where they are [29], [30]. Adding fully connected layer is an inexpensive way to teach non-linear components of these properties. Most of the properties extracted from the two layers of convolution and pooling may be suitable for classification. Still, the compounds composed of these properties may be better, and the sum of the probabilities extracted from the fully connected layer is equal to the value one.

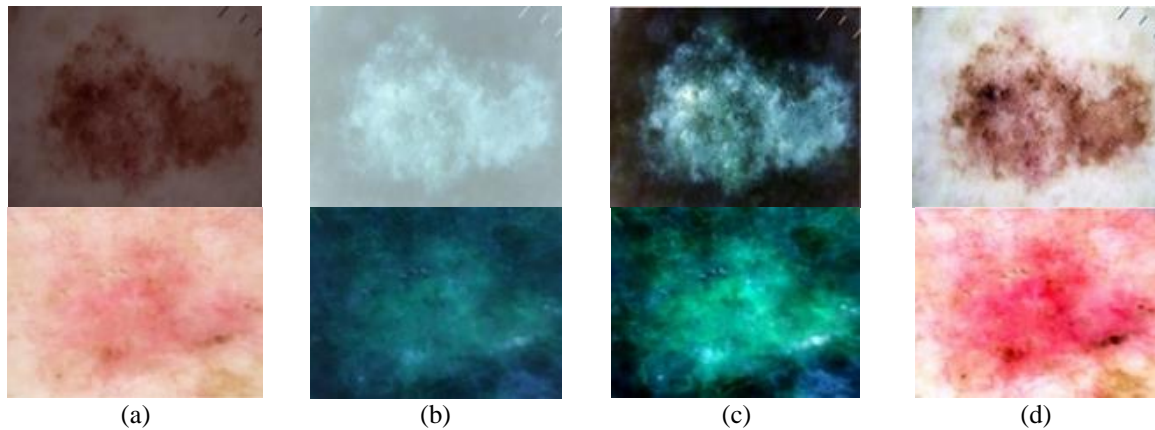


Figure 3. Enhancing dark and bright images (a) luminous and dark original images, (b) invert the images, (c) apply enhancing algorithm, and (d) invert the enhanced images

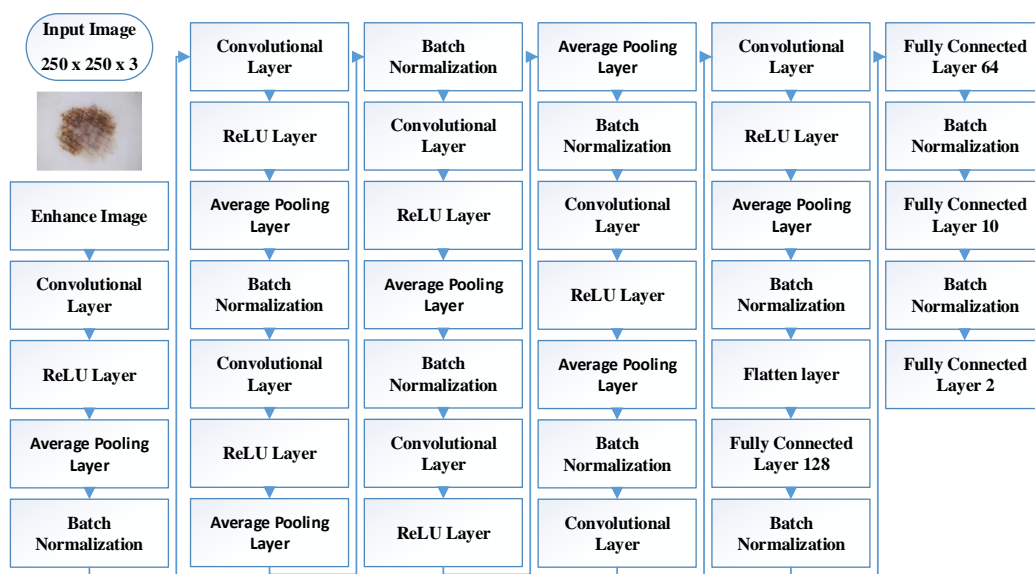


Figure 4. The proposed architecture of the training process

The convolutional neural network architecture design and construction are characterized by the fact that it deals with digital images based on two essential bases: dealing with the different textures of digital images and the various colors of the entities within the digital images. In the proposed architecture, the tissues of images of skin diseases were dealt with in the stage of convolution. Figure 5 shows images of a skin disease that contains hair, where is Figures 5(a)-(c) they explain texture analysis of skin disease images, and Figure 5(d)-(f) they explain various colors for skin diseases. When convolution is applied, the tissues of the disease and the tissues of hair are distinguished. In this case, disease-specific features and features of the surrounding noise are obtained. The diversity of colors for skin diseases gave it a unique advantage by collecting colors and considering them as distinctive characteristics added to the features used in the classification process based on pooling operations.

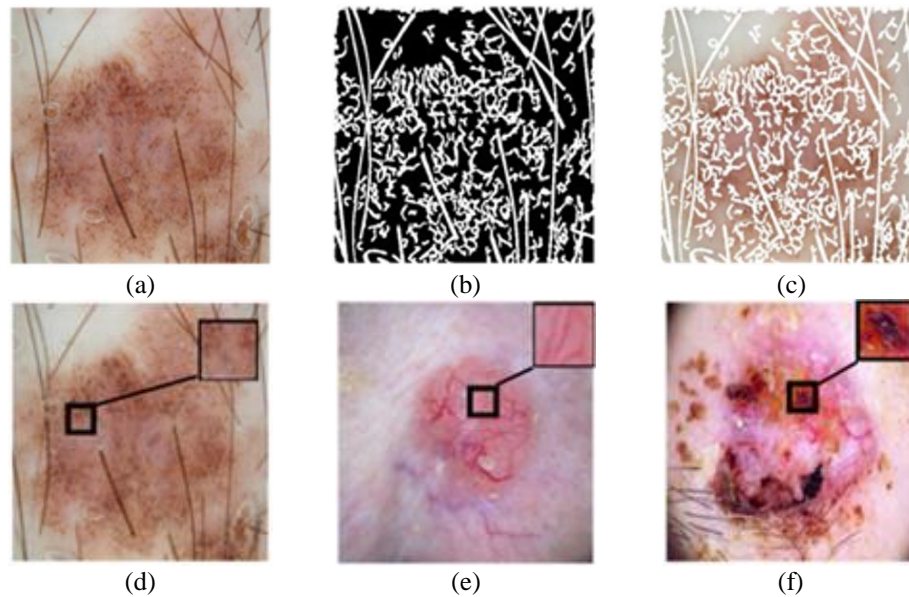


Figure 5. Diversity of shapes and colors of skin diseases (a), (b), (c) texture analysis of skin disease images, (d), (e), (f) various colors for skin diseases

4. RESEARCH METHOD

The convolution and the pooling layers act as an extract of the properties from the input image. The fully connected layer works as a classifier for the input image using the extracted properties, as in Figure 6. The target class in the output is equal to one. At the same time, it is similar to zero for the rest of the types, and the convolution network training process can be summarized in the following steps:

- i) Insert the filters to be used and select parameters and weights from random values.
- ii) Insert training images into the network with finding the output potential for each class through forwarding propagation (convolution operations, ReLU, Pooling, forward propagation of the fully connected layer).
 - Assuming the probability of outputting the image is [0.3, 0.5, 0.2, 0.3].
 - The resulting probability of the first training sample will be random because the initial weight will be random.
- iii) Calculate the total error in the output layer, as in (3):

$$\text{Total Error} = \sum \frac{1}{2}(X - Y)^2 \quad (3)$$

where X=target probability, Y=output probability.

- iv) Use the backpropagation algorithm to calculate the error gradient according to the weight of the grid.
 - Weight update is affected by the total error.
 - The output probability of [0.2, 0.2, 0.8, 0.2] is nearest to the target vector [0, 0, 1, 0] for the same input image. This indicates that the network can classify this image by adjusting the filters and weights correctly.

- The filter matrix value and weights are updated and the number of filters, filter size, network structure, and other parameters are fixed.
- v) Repeat steps 1 through 4 for all images in the training data.
- vi) When a new (invisible) image is used as an input to the network, the network will perform the forward propagation process again and output the probabilities of each class (for the new image, the likelihood of output is improved over the previous training samples). If the training dataset is too large, the network will generalize the latest images and categorize them into the correct categories.

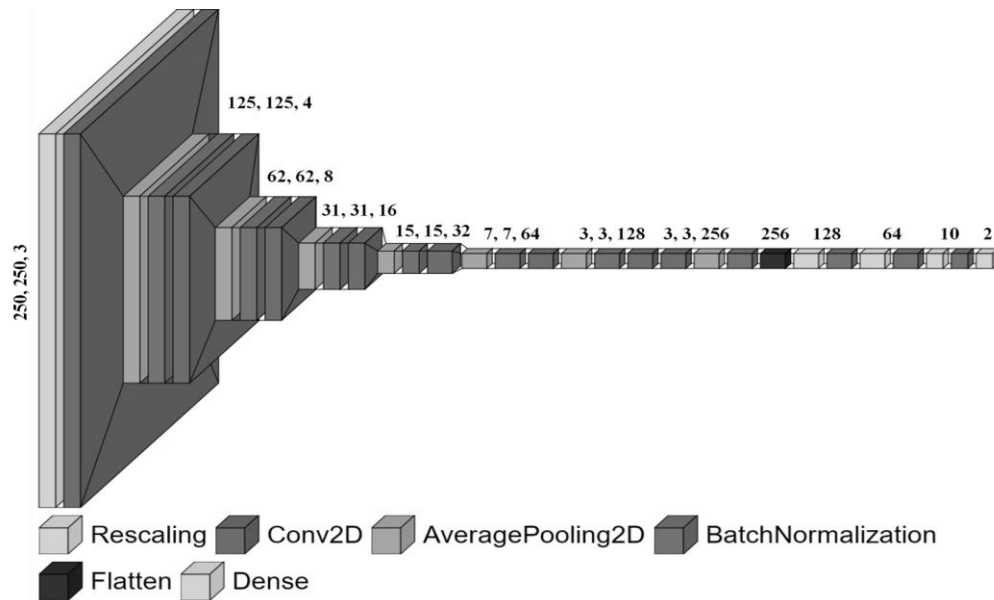


Figure 6. Steps to implement the proposed convolutional neural network

5. RESULTS AND DISCUSSION

Various skin disease image samples were dealt with as in Figure 7 shows images of BCC that were taken in different shapes and colors, as two malignant skin diseases were detected, each separately compared to nevus images. It was found through the detection process that the accuracy of classification with BCC disease was higher than the classification accuracy with melanoma disease as shown in Figure 8, where is Figure 8(a) Shows BCC detection and Figure 8(b) Shows melanoma detection. Noting that the images of normal nevus are the same were applied to the two diseases and as shown in Tables 1 and 2. The essential feature of the proposed architecture is reaching the high accuracy of classification through the training process. By observing Figure 8, it is clear that the number of the epoch is 50, while the required accuracy was reached before that. The proposed architecture has also been adapted to deal with various images, different in shape and color, and the method of capturing the image of the disease.

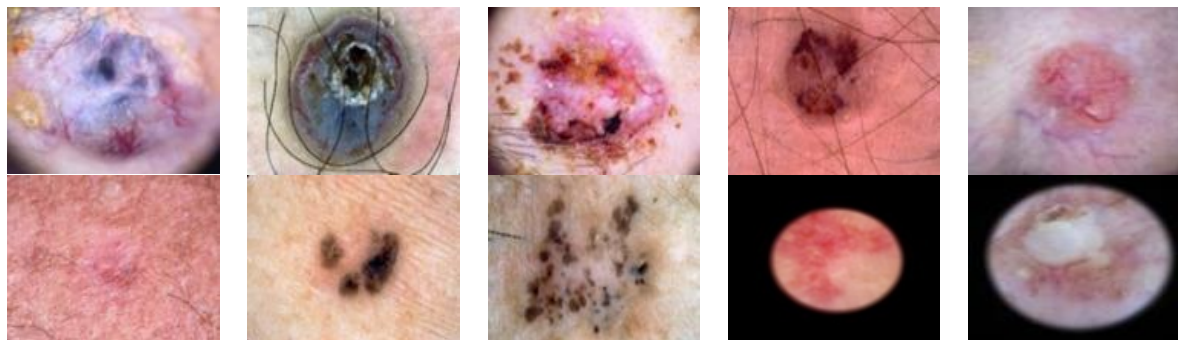


Figure 7. Various basal cell carcinomas

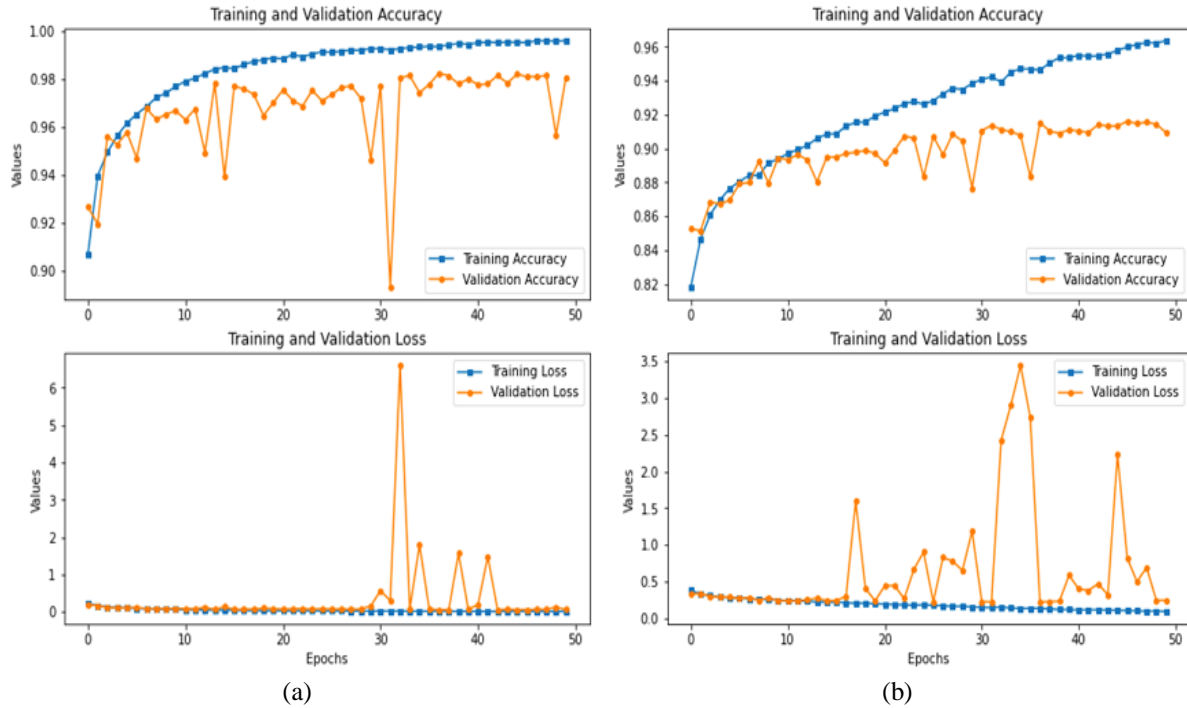


Figure 8. Results of training and verification processes (a) BCC detection and (b) melanoma detection

Table 1. Accuracy for detecting BCC disease

Architecture	Total No. of Layers	Conv. Layers	FC Layers	Samples	No. of Images (The ISIC Archive 2020)	Time for 50 epoch	Accuracy
LeNet-5	5	2	3	Nevus	9566	CPU=158 Min	94.66 %
				BCC	3008	GPU=17 Min	
AlexNet	8	5	3	Nevus	9566	CPU=183 Min	87.63 %
				BCC	3008	GPU=20 Min	
ZFNet	8	5	3	Nevus	9566	CPU=191 Min	76.41 %
				BCC	3008	GPU=21 Min	
VGG-16	16	13	3	Nevus	9566	CPU=291 Min	76.51 %
				BCC	3008	GPU=32 Min	
A Proposed Architecture of CNN	12	8	4	Nevus	9566	CPU=666 Min	98.25 %
				BCC	3008	GPU=74 Min	

Table 2. Accuracy for detecting melanoma disease

Architecture	Total No. of Layers	Conv. Layers	FC Layers	Samples	No. of Images (The ISIC Archive 2020)	Time for 50 epoch	Accuracy
LeNet-5	5	2	3	Nevus	9566	CPU=160 Min	88.51 %
				Melanoma	5272	GPU=19 Min	
AlexNet	8	5	3	Nevus	9566	CPU=185 Min	81.16 %
				Melanoma	5272	GPU=22 Min	
ZFNet	8	5	3	Nevus	9566	CPU=193 Min	64.73 %
				Melanoma	5272	GPU=23 Min	
VGG-16	16	13	3	Nevus	9566	CPU=293 Min	63.94 %
				Melanoma	5272	GPU=34 Min	
Proposed Architecture of CNN	12	8	4	Nevus	9566	CPU=668 Min	91.61 %
				Melanoma	5272	GPU=76 Min	

6. CONCLUSION

The accuracy rate in differentiation processes varies according to the data used and the similarity between that data. The results showed that the accuracy rate in detecting BCC disease was higher than the detection rate of melanoma disease. However, the percentage of accuracy in detecting both diseases was high. Also, the proposed architecture used in this research showed high efficiency in detecting malignant diseases. The accuracy ratio increases as the training steps increase (epoch), unlike some other architectures. They gain a constant accuracy that does not improve with the increase in training steps (epoch). This feature

increased the efficiency of the testing process concerning the randomly selected images for testing by obtaining high accuracy in the discrimination process. The proposed project is characterized by exemplary performance and high resolution of many of the images that were dealt with, and the significant difference between one image and another regarding the different shapes and colors of these diseases. AI-architecture also gave typical results with many input images, as the images were taken from the ISIC 2020 archive.




REFERENCES

- [1] A. M. Alkabaji and O. H. Mohammed, "Real time ear recognition using deep learning," *Telecommunication Computing Electronics and Control (TELKOMNIKA)*, vol. 19, no. 2, pp. 523–530, Apr. 2021, doi: 10.12928/telkomnika.v19i2.18322.
- [2] M. Alenezi, M. Akour, and O. Al Qasem, "Harnessing deep learning algorithms to predict software refactoring," *Telecommunication Computing Electronics and Control (TELKOMNIKA)*, vol. 18, no. 6, pp. 2977–2982, Dec. 2020, doi: 10.12928/telkomnika.v18i6.16743.
- [3] M. Ghazal, N. Waisi, and N. Abdullah, "The detection of handguns from live-video in real-time based on deep learning," *Telecommunication Computing Electronics and Control (TELKOMNIKA)*, vol. 18, no. 6, p. 3026, Dec. 2020, doi: 10.12928/telkomnika.v18i6.16174.
- [4] A.-R. Ali, J. Li, G. Yang, and S. J. O'Shea, "A machine learning approach to automatic detection of irregularity in skin lesion border using dermoscopic images," *PeerJ Computer Science*, vol. 6, Jun. 2020, Art. no. e268, doi: 10.7717/peerj-cs.268.
- [5] G. A. Shadeed, M. A. Tawfeeq, and S. M. Mahmoud, "Deep learning model for thorax diseases detection," *Telecommunication Computing Electronics and Control (TELKOMNIKA)*, vol. 18, no. 1, pp. 441–449, Feb. 2020, doi: 10.12928/telkomnika.v18i1.12997.
- [6] S. P., O. V. Ramana Murthy, and S. Veni, "Sentiment analysis by deep learning approaches," *Telecommunication Computing Electronics and Control (TELKOMNIKA)*, vol. 18, no. 2, pp. 752–760, Apr. 2020, doi: 10.12928/telkomnika.v18i2.13912.
- [7] A. Esteva *et al.*, "Deep learning-enabled medical computer vision," *npj Digital Medicine*, vol. 4, no. 1, Dec. 2021, Art. no. 5, doi: 10.1038/s41746-020-00376-2.
- [8] M. A. Kassem, K. M. Hosny, and M. M. Fouad, "Skin lesions classification into eight classes for ISIC 2019 using deep convolutional neural network and transfer learning," *IEEE Access*, vol. 8, pp. 114822–114832, 2020, doi: 10.1109/ACCESS.2020.3003890.
- [9] M. K. Monika, N. Arun Vignesh, C. Usha Kumari, M. N. V. S. S. Kumar, and E. L. Lydia, "Skin cancer detection and classification using machine learning," *Materials Today: Proceedings*, vol. 33, pp. 4266–4270, 2020, doi: 10.1016/j.matpr.2020.07.366.
- [10] E. Yilmaz and M. Trocan, "A modified version of GoogLeNet for melanoma diagnosis," *Journal of Information and Telecommunication*, vol. 5, no. 3, pp. 395–405, Jul. 2021, doi: 10.1080/24751839.2021.1893495.
- [11] J. Saeed and S. Zeebaree, "Skin lesion classification based on deep convolutional neural networks architectures," *Journal of Applied Science and Technology Trends*, vol. 2, no. 01, pp. 41–51, Mar. 2021, doi: 10.38094/jastt20189.
- [12] V. M. M., "Melanoma skin cancer detection using image processing and machine learning," *International Journal of Trend in Scientific Research and Development*, vol. 3, no. 4, pp. 780–784, Jun. 2019, doi: 10.31142/ijtsrd23936.
- [13] S. Syedhusain, S. Vairaprakash, R. D. Nayagam, K. Mahendran, and S. Sakthimani, "MDCNN-modified deep convolutional neural network system for classifying COVID-19 image dataset," *Annals of R. S. C. B.*, vol. 25, no. 5, pp. 1667–1680, 2021.
- [14] U. R. Chowdhury, S. Jana, and R. Parekh, "Automated system for indian banknote recognition using image processing and deep learning," in *2020 International Conference on Computer Science, Engineering and Applications (ICCSEA)*, Mar. 2020, pp. 1–5, doi: 10.1109/ICCSEA49143.2020.9132850.
- [15] B. Gao, X. Li, W. L. Woo, and G. Yun Tian, "Physics-based image segmentation using first order statistical properties and genetic algorithm for inductive thermography imaging," *IEEE Transactions on Image Processing*, vol. 27, no. 5, pp. 2160–2175, May 2018, doi: 10.1109/TIP.2017.2783627.
- [16] J. Boman and A. Volminger, "Evaluating a deep convolutional neural network for classification of skin cancer Evaluating a deep convolutional neural network for classification of skin cancer," pp. 1–30, 2018.
- [17] V. Rotemberg *et al.*, "A patient-centric dataset of images and metadata for identifying melanomas using clinical context," *Scientific Data*, vol. 8, no. 1, Dec. 2021, Art. no. 34, doi: 10.1038/s41597-021-00815-z.
- [18] T.-C. Pham, C.-M. Luong, M. Visani, and V.-D. Hoang, "Deep CNN and data augmentation for skin lesion classification," in *Lecture Notes in Computer Science (including subseries Lecture Notes in Artificial Intelligence and Lecture Notes in Bioinformatics)*, vol. 10752 LNAI, no. January, 2018, pp. 573–582.
- [19] S. Jinnai, N. Yamazaki, Y. Hirano, Y. Sugawara, Y. Ohe, and R. Hamamoto, "The development of a skin cancer classification system for pigmented skin lesions using deep learning," *Biomolecules*, vol. 10, no. 8, Jul. 2020, Art. no. 1123, doi: 10.3390/biom10081123.
- [20] X. Dong, Y. (Amy) Pang, and J. (Gene) Wen, "Fast efficient algorithm for enhancement of low lighting video," in *ACM SIGGRAPH 2010 Posters on-SIGGRAPH '10*, 2010, Art. no. 1, doi: 10.1145/1836845.1836920.
- [21] T. Gao and G. Y. Wang, "Brain signal classification based on deep CNN," *International Journal of Security and Privacy in Pervasive Computing*, vol. 12, no. 2, pp. 17–29, Apr. 2020, doi: 10.4018/IJSPPC.2020040102.
- [22] A. Maiti and B. Chatterjee, "Improving detection of Melanoma and Naevus with deep neural networks," *Multimedia Tools and Applications*, vol. 79, no. 21–22, pp. 15635–15654, Jun. 2020, doi: 10.1007/s11042-019-07814-8.
- [23] A. A. Mohamed, W. A. Mohamed, and A. H. Zekry, "Deep learning can improve early skin cancer detection," *International Journal of Electronics and Telecommunications*, vol. 65, no. 3, 2019.
- [24] A. Mikolajczyk and M. Grochowski, "Data augmentation for improving deep learning in image classification problem," in *2018 International Interdisciplinary PhD Workshop (IIPHDW)*, May 2018, pp. 117–122, doi: 10.1109/IIPHDW.2018.8388338.
- [25] S. C. Wong, A. Gatt, V. Stamatescu, and M. D. McDonnell, "Understanding data augmentation for classification: when to warp?," in *2016 International Conference on Digital Image Computing: Techniques and Applications (DICTA)*, Nov. 2016, pp. 1–6, doi: 10.1109/DICTA.2016.7797091.
- [26] M. A. Kadampur and S. Al Riyae, "Skin cancer detection: Applying a deep learning based model driven architecture in the cloud for classifying dermal cell images," *Informatics in Medicine Unlocked*, vol. 18, 2020, Art. no. 100282, doi: 10.1016/j.imu.2019.100282.
- [27] P. Wanda, M. E. Hiswati, and H. J. Jie, "DeepOSN: Bringing deep learning as malicious detection scheme in online social




- network,” *IAES International Journal of Artificial Intelligence (IJ-AI)*, vol. 9, no. 1, pp. 146–154, Mar. 2020, doi: 10.11591/ijai.v9.i1.pp146-154.
- [28] P. N. Srinivasu, J. G. SivaSai, M. F. Ijaz, A. K. Bhoi, W. Kim, and J. J. Kang, “Classification of skin disease using deep learning neural networks with MobileNet V2 and LSTM,” *Sensors*, vol. 21, no. 8, Apr. 2021, Art. no. 2852, doi: 10.3390/s21082852.
- [29] H. M. Son *et al.*, “AI-based localization and classification of skin disease with erythema,” *Scientific Reports*, vol. 11, no. 1, Dec. 2021, Art. no. 5350, doi: 10.1038/s41598-021-84593-z.
- [30] J. Steppan and S. Hanke, “Analysis of skin lesion images with deep learning.” Jan. 11, 2021, Available: <http://arxiv.org/abs/2101.03814>.

BIOGRAPHIES OF AUTHORS



Hasan Maher Ahmed    obtained his M.Sc. degree in Computer Science from the University of Mosul, Mosul, Iraq in 2009. His main field of interest are Image Processing, Artificial Intelligence, and Computer Vision. He can be contacted at email: hasanmaher@uomosul.edu.iq.



Manar Younis Kashmola    obtained her Ph.D. degree in Computer Science from the University of Mosul, Iraq in 2004. She is currently a computer science professor at Ninevah University, Iraq. She is also a Chairman of the Board of Directors of the Advisory Office at the University of Mosul. Her main fields of interest are Computer Networks, Distributed Systems, Wireless Communication. She can be contacted at email: Manar.kashmola@uomosul.edu.iq.